Modeling the Evolution of PAH abundance in galaxies

Shiau-Jie Rau
National Tsing Hua University
Hiroyuki Hirashita
Institute of Astronomy and Astrophysics, Academia Sinica
Maria Murga
Institute of Astronomy, Russian Academy of Sciences

PAH
Polycyclic Aromatic Hydrocarbons

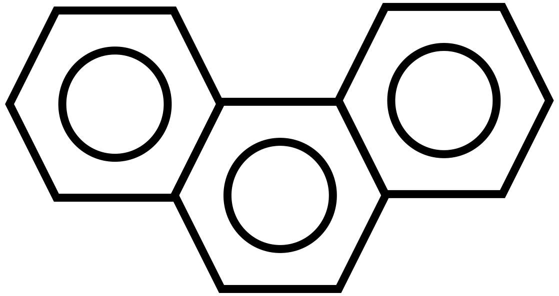

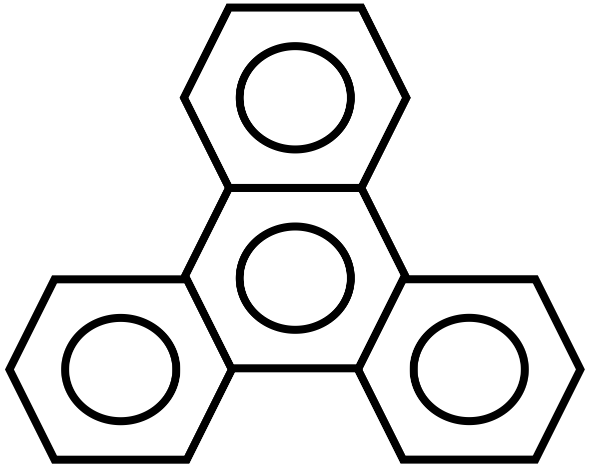

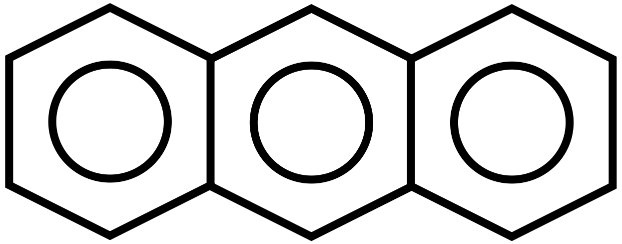

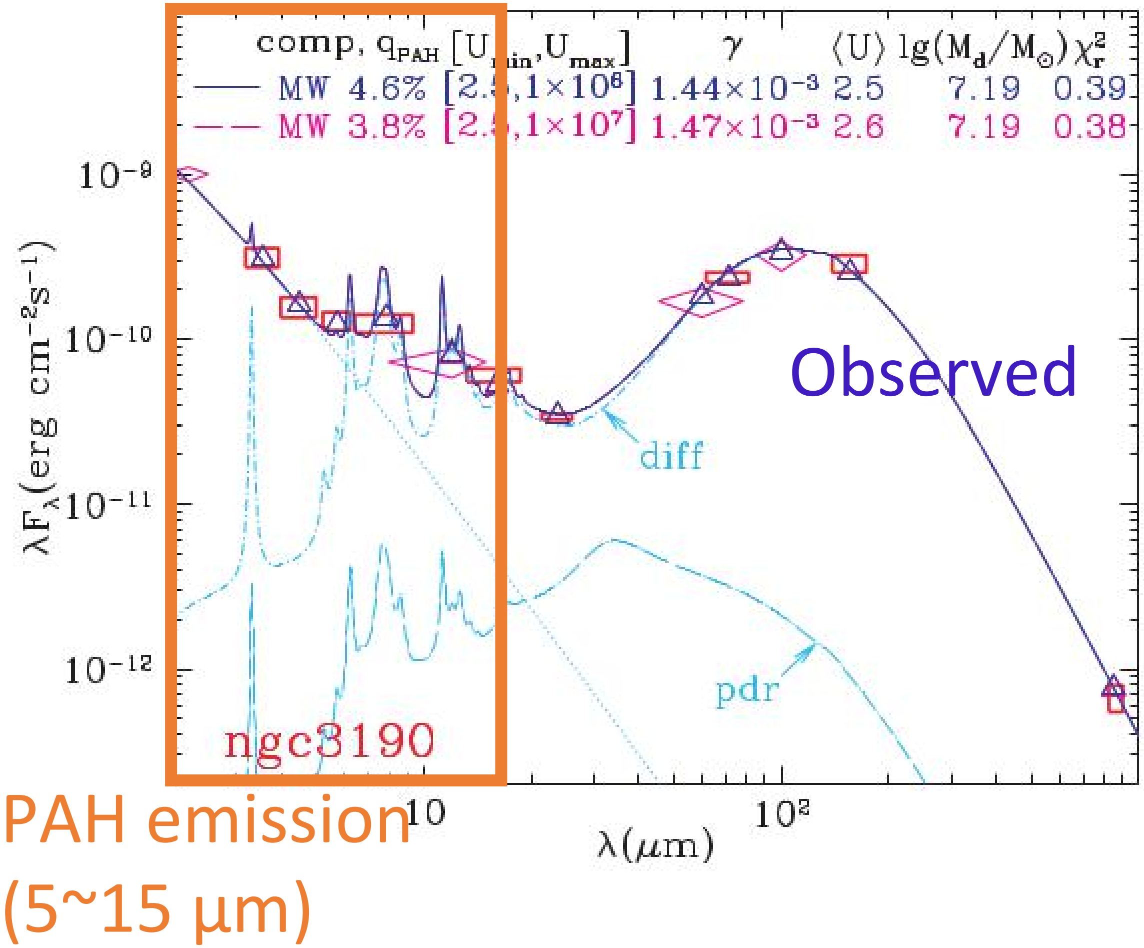

Size range: 0.0003 μm ~ 0.002 μm

Draine et al. 2007

- The PAH spectrum intensity has a strong correlation with metallicity. (Engelbracht et al. 2005)
- This correlation was explained by assuming that PAHs are formed by shattering of large carbonaceous grains. (Seok et al. 2014)

We want to consider grain size evolution in a self-consistent model.

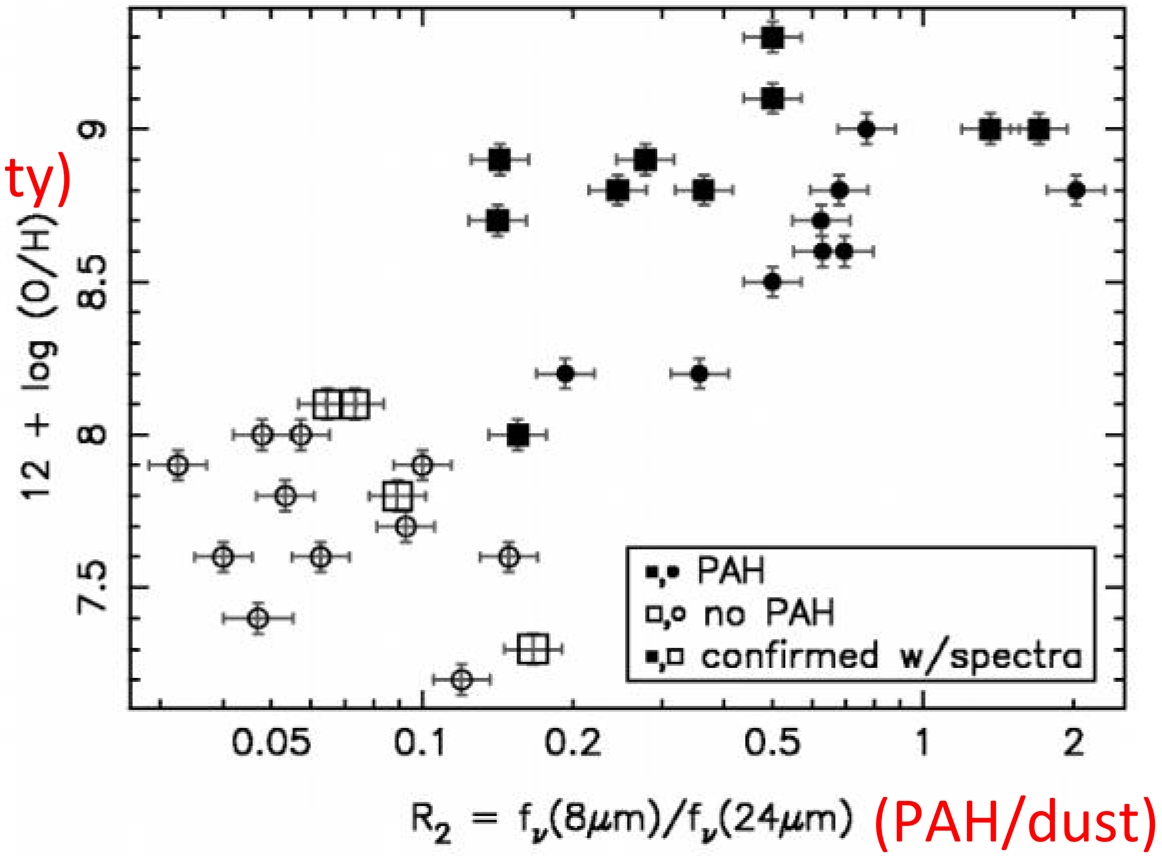

FIG. 2.—Galaxy metallicity as a function of the 8-to-24 μm color. Galaxies with colors or spectra that indicate that they have 8 μm PAH features are displayed as filled symbols, while galaxies that lack the 8 μm PAH feature are shown as open symbols. Squares and circles denote measurements with and without spectroscopic confirmation, respectively. The error bars on the 8-to-24 μm ratio are the same as in Fig. 1, while the error bars on the metallicity are typically 0.05 or less (cf. Kobulnicky & Skillman 1996) and were all assigned an uncertainty of 0.05. Note that this figure does not require IRAC data (some of the 8 μm measurements were made by *MSX*) and thus contains more points than Fig. 1.

Engelbracht et al. 2005

Theoretical Model Included

- Post-processed Hydrodynamics Simulation
- Grain Size Distribution (Dust Evolution Process)
- Aromatization

Post-Processed Hydrodynamics Simulation

- GADGET-3-osaka N-body/smoothed particle hydrodynamics (SPH) simulation for an isolated galaxy
- Post-processing 149 SPH particles based on metallicity, temperature, and density evolution

We can consider different evolutional path!!!

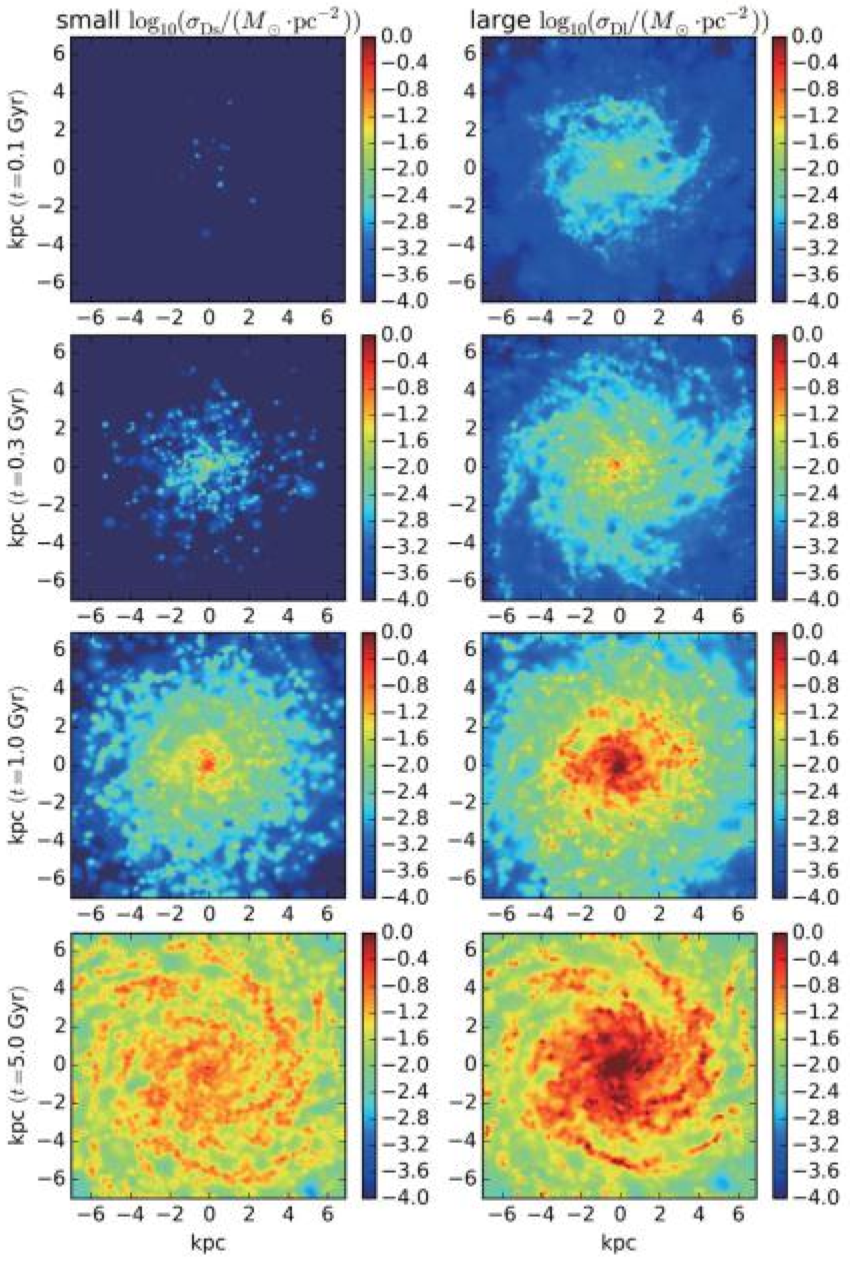

Figure 3. Face-on view of the surface densities of small grains (left-hand column) and large grains (right-hand column) at $t = 0.1$, 0.3, 1 and 5 Gyr (top to bottom).

Aoyama et al. 2016

Grain Size Distribution (Dust evolution Processes)

Hirashita et al. 2019

→ Solved on each SPH particle

Stellar Dust Production

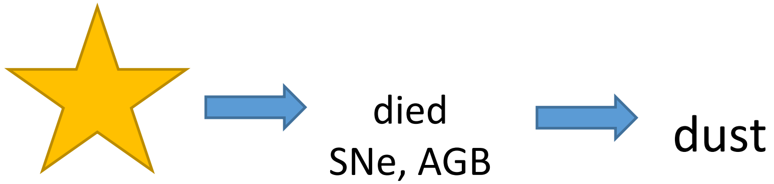

Diffuse

$1.0cm^{-3} > n_{\mathrm{H}} > 0.1cm^{-3},\ 10^{4}K > T_{\mathrm{gas}} > 10^{3}\mathrm{K}$

Sputtering

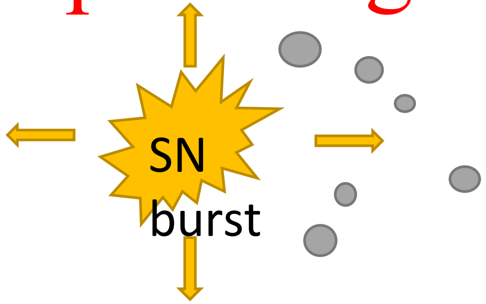

Large grains becom
smaller,
small grains disappear

Shattering

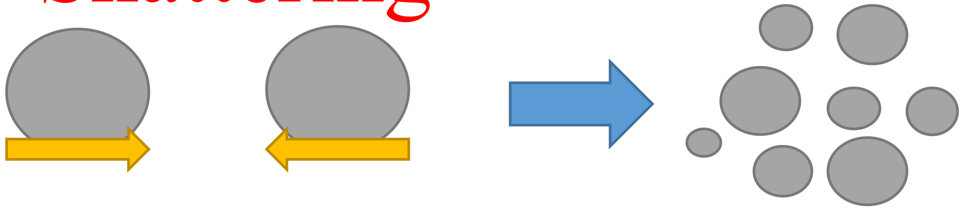

Dense

$n_{\mathrm{H}} > 10cm^{-3},\ T_{\mathrm{gas}} < 10^{3}\mathrm{K}$

Coagulation

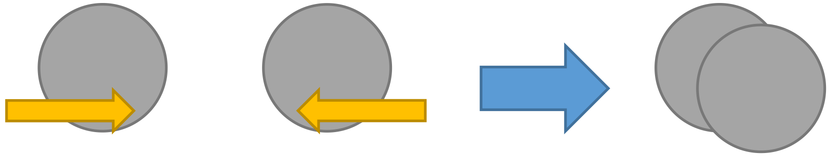

Accretion

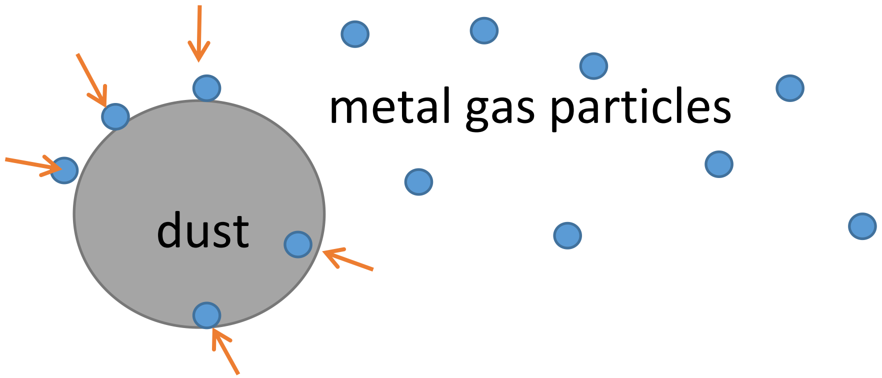

Simulation Process

(Only carbonaceous grains are considered for simplicity)

Non-aromatic carbon dust

1. stellar dust production
2. shattering
3. coagulation
4. accretion
5. sputtering

$$\frac{\tau_{\rm ar}}{\rm yr} = 3\left(\frac{a}{\mu{\rm m}}\right)^{-2} + 6.6\times10^{7}\left(\frac{a}{\mu{\rm m}}\right)$$

aromatization

Derived by aromatization caused by UV irradiation reaction

Hydrogen density: $0.1\ {\rm cm}^{-3} < n_{\rm H} < 1\ {\rm cm}^{-3}$

Aromatic carbon dust

1. shattering
2. coagulation
3. sputtering

PAH size range:

0.0003 μm ~ 0.002 μm

PAH

Grain Size Distribution

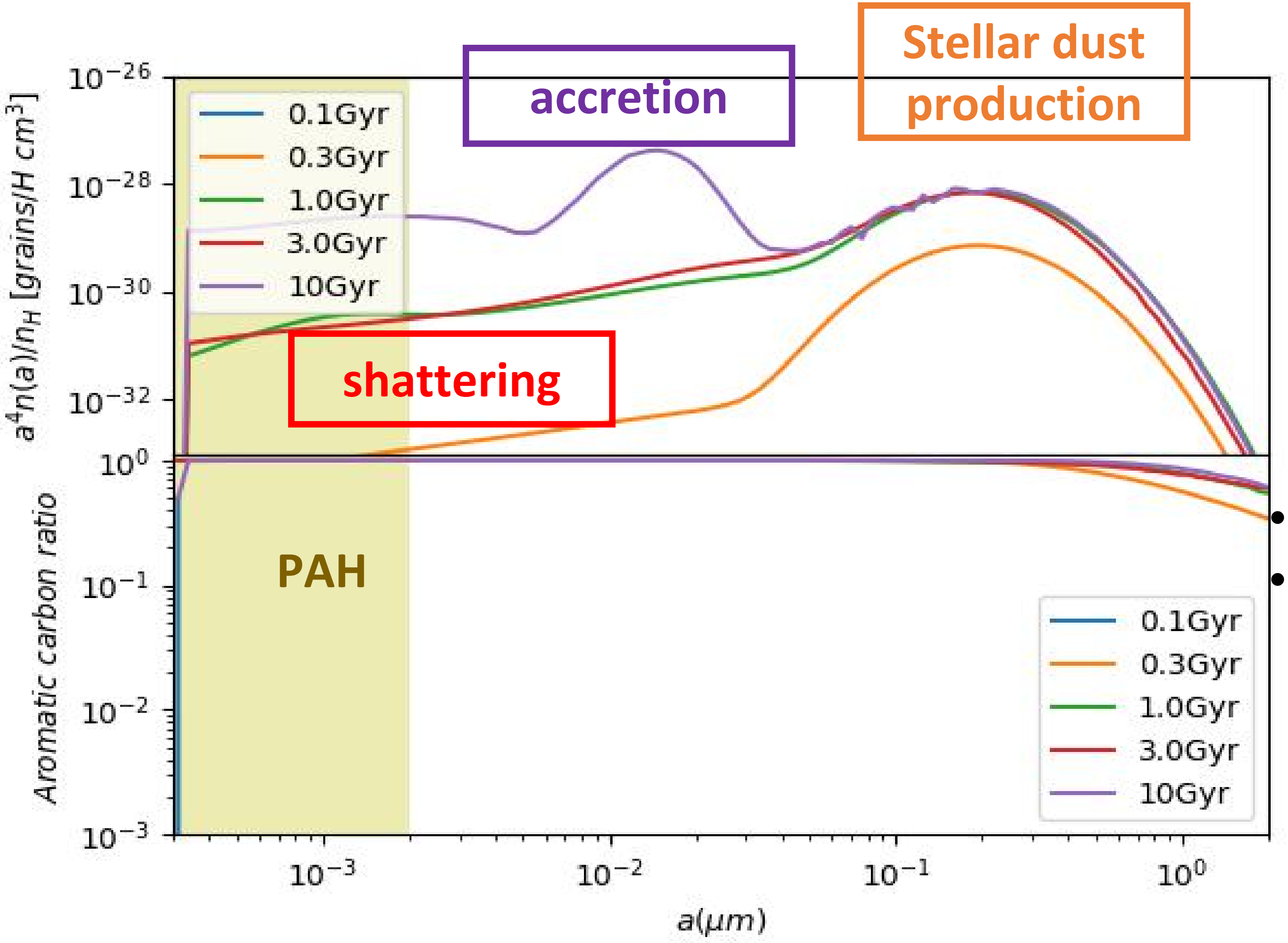

- **Small grains are aromatized**
- **Shattering and accretion are important for PAH abundancce**

PAH abundance vs. metallicity

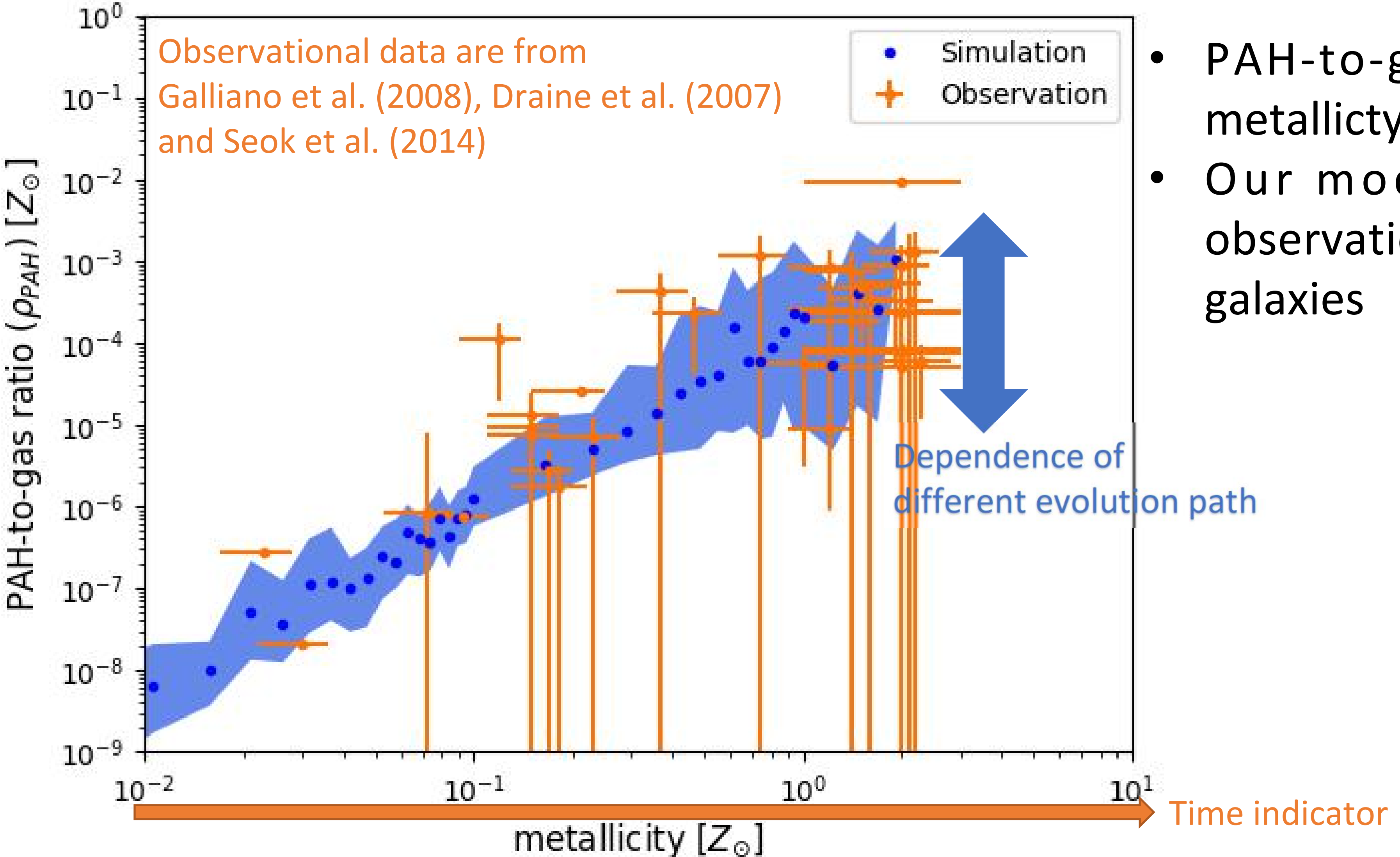

- PAH-to-gas ratio increases with metallicty
- Our model is consistent with observational data points of nearby galaxies

PAH-to-dust mass ratio v.s metallicity

Observational data are from
Galliano et al. (2008), Draine et al. (2007)
and Seok et al. (2014)

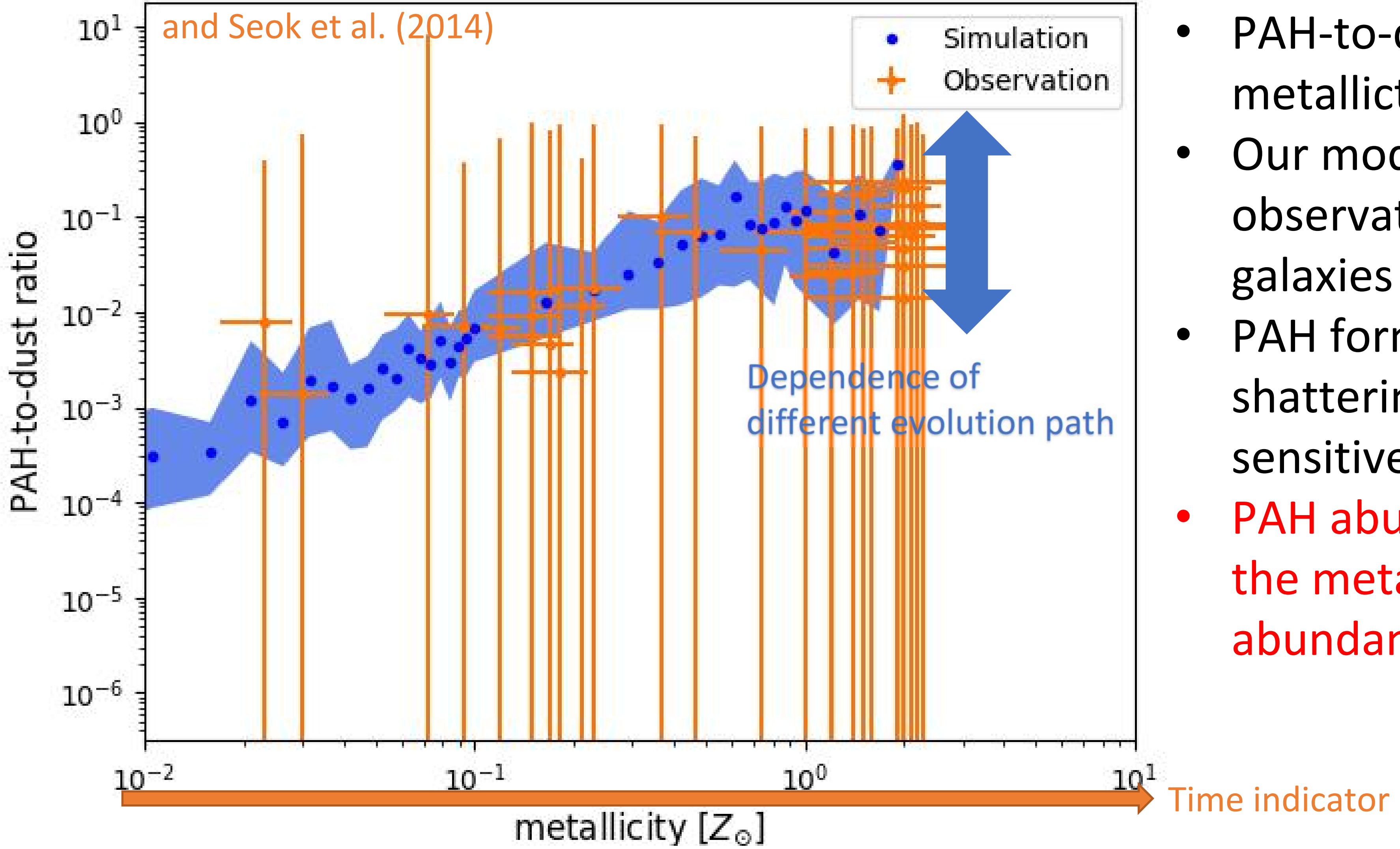

- PAH-to-dust ratio increases with metallicty
- Our model is consistent with observational data points of nearby galaxies
- PAH formation is dominated by shattering and accretion, which are sensitive to metallicity
- PAH abundance is more sensitive to the metallicity than the total dust abundance is.

Conclusion

- PAH abundance evolution is formulated taking grain size distribution and aromatization into account.
- By post-processing a hydrodynamical simulation of an isolated galaxy, we succeed in explaining the relation between PAH abundance and metallicity
- PAH abundance is more sensitive to the metallicity than the total dust abundance

Thank you

Dust-to-gas ratio vs. metallicity

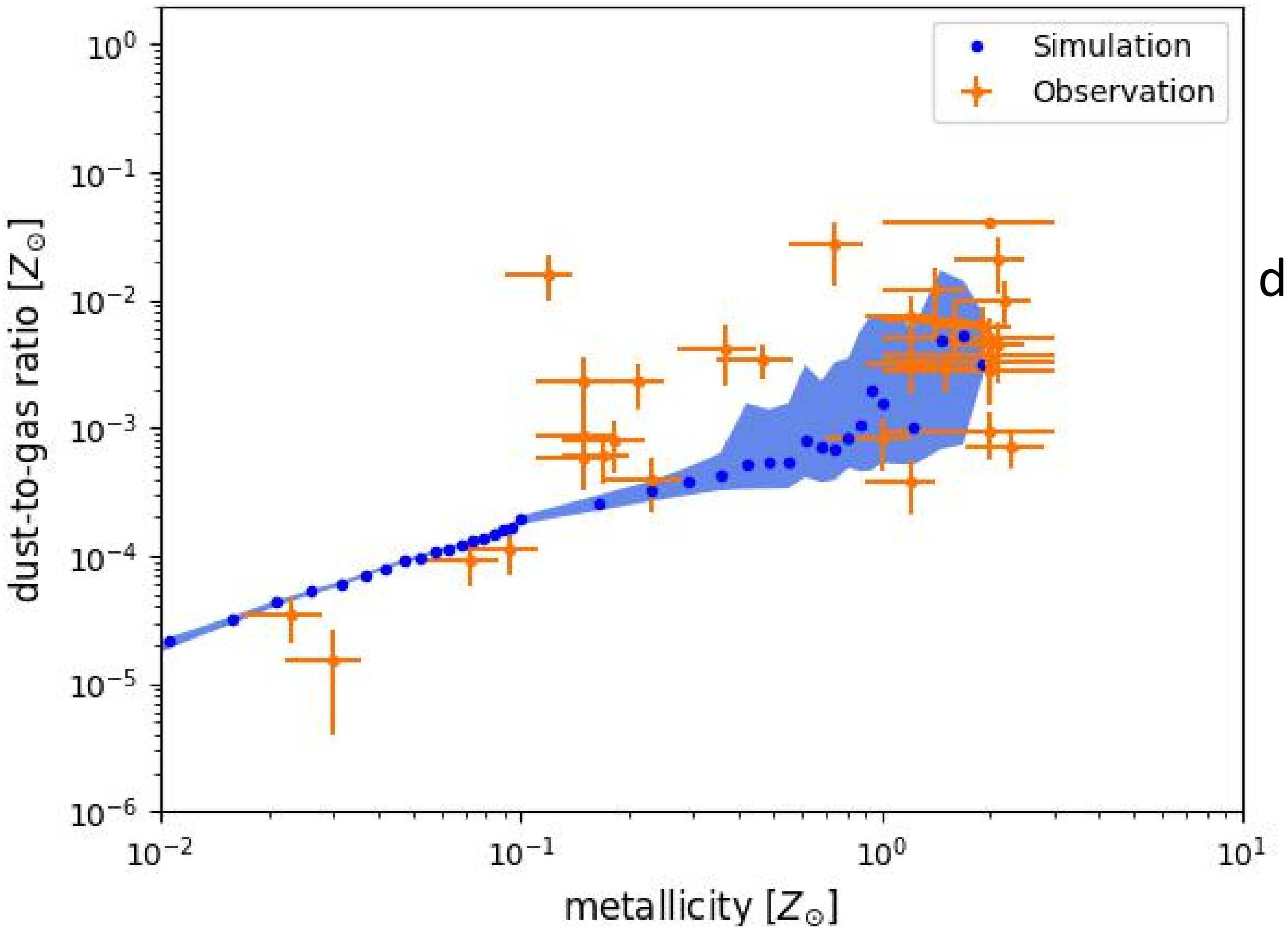

dust-to-gas ratio increases with metallicty

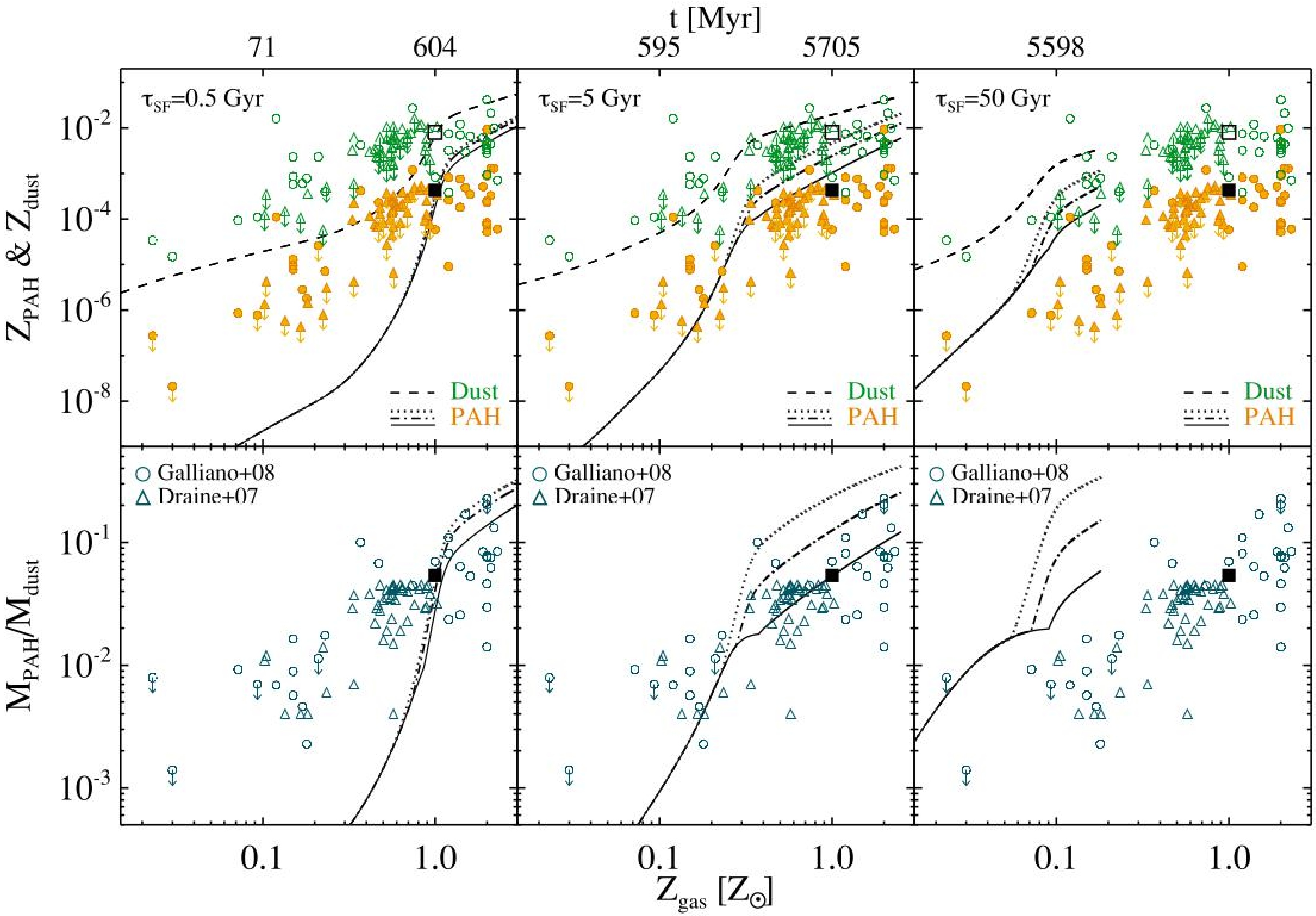

Figure 5. Top: calculated PAH-to-gas mass ratio ($Z_{\rm PAH}$) and dust-to-gas ratio ($Z_{\rm dust}$, dashed line) as a function of metallicity ($Z_{\rm gas}$) for $\tau_{\rm SF} = 0.5$, 5, and 50 Gyr. As for $Z_{\rm PAH}$, the cases for $\tau_{\rm DC} = 1$, 3, and 10 Myr are overlaid in each panel with solid, dash–dotted, and dotted lines, respectively. Observational data from Galliano et al. (2008) and Draine et al. (2007) are overlaid for comparison (circles and triangles, respectively). $Z_{\rm dust}$ and $Z_{\rm PAH}$ are distinguished with open and filled symbols. Also, $Z_{\rm PAH}$ and $Z_{\rm dust}$ of the diffuse Galactic ISM are denoted with filled and open squares, respectively (Zubko et al. 2004). The time corresponding to the metallicity are indicated on the top axis. As the model calculation terminates at 10 Gyr, the time at $Z_{\rm gas} = 1$ cannot be marked in the case of $\tau_{\rm SF} = 50$ Gyr. Bottom: total mass ratio of PAH to dust ($Z_{\rm PAH}/Z_{\rm dust}$) for $\tau_{\rm SF} = 0.5$, 5, and 50 Gyr.

Stellar dust production

total mass density (including gas and dust)

$$\frac{\partial \rho_{dust}}{\partial t} = f_{in} \dot{\rho}_z m \widetilde{\varphi}(m)$$

condensation efficiency for metals (= 0.1)

mass distribution function (lognormal distribution centure at a= 0.1μm)

m: single dust particle mass, m=m(a)

Sputtering (Super nova destruction)

$$\tau_{\rm dest}(m) = \frac{M_{\rm gas}}{\epsilon_{\rm dest}(m) M_{\rm s} \gamma}$$

destruction efficiency

$$\epsilon_{\rm dest}(a) = 1 - \exp\left[-0.1\left(\frac{a}{0.1\,\mu{\rm m}}\right)\right]$$

Accretion

$$\tau'_{\rm acc}(a) = \tau'_{0,\rm acc}\left(\frac{a}{0.1\,\mu\rm m}\right)\left(\frac{Z}{Z_\odot}\right)^{-1}\left(\frac{n_{\rm H}}{10^3\,\rm cm^{-3}}\right)^{-1} \times \left(\frac{T_{\rm gas}}{10\,\rm K}\right)^{-1/2}\left(\frac{S}{0.3}\right)^{-1}$$

Sticking probibility: S = 0.3

Shattering

$$\left[\frac{\partial \rho_{\mathrm{d}}(m,\, t)}{\partial t}\right]_{\mathrm{shat}} = -m\rho_{\mathrm{d}}(m,\, t)\int_0^\infty \alpha(m_1,\, m)\rho_{\mathrm{d}}(m_1,\, t)\,\mathrm{d}m_1$$

$$+ \int_0^\infty \int_0^\infty \alpha(m_1,\, m_2)\rho_{\mathrm{d}}(m_1,\, t)\rho_{\mathrm{d}}(m_2,\, t)$$

$$\times\, \mu_{\mathrm{frag}}(m;\, m_1,\, m_2)\mathrm{d}m_1\mathrm{d}m_2,$$

probability to collision

proportional to metallicity

Coagulation

probability to collision

$$\left[\frac{\partial \rho_{\rm d}(m,\, t)}{\partial t}\right]_{\rm coag} = -m\rho_{\rm d}(m,\, t)\int_0^\infty \underline{\alpha(m_1,\, m)}\underline{\rho_{\rm d}(m_1,\, t)}\, {\rm d}m_1$$

$$+ \int_0^\infty \int_0^\infty \underline{\alpha(m_1,\, m_2)}\underline{\rho_{\rm d}(m_1,\, t)\rho_{\rm d}(m_2,\, t)}$$

$$\times\, m_1 \delta(m - m_1 - m_2)\, {\rm d}m_1 {\rm d}m_2 .$$

proportional to metallicity